Time–temperature–transformation diagram and microstructures of bulk glass forming $Pd_{40}Cu_{30}Ni_{10}P_{20}$

Jörg F. Löffler,[a] Jan Schroers, and William L. Johnson
W. M. Keck Laboratory, California Institute of Technology, Pasadena, California 91125

(Received 7 April 2000; accepted for publication 6 June 2000)

Isothermal crystallization studies were performed on the bulk glass forming alloy $Pd_{40}Cu_{30}Ni_{10}P_{20}$ in the undercooled liquid region between the glass transition and liquidus temperature, resulting in a complete time–temperature–transformation (TTT) diagram for crystallization. The TTT diagram shows a typical ''C'' shape with the nose at 50 s and 680 K. Assuming steady state nucleation and a diffusion-controlled growth rate, the TTT diagram was successfully fit over the entire range of the measurement. The microstructure after isothermal crystallization shows a modulation in Cu and P for all degrees of undercooling. The primary solidified phase is Cu_3Pd, which forms distinct dendrites at low undercooling. From additional constant cooling experiments, the critical cooling rate to bypass crystallization was determined to be 0.33 K/s. © *2000 American Institute of Physics.* [S0003-6951(00)02231-2]

In 1984, it was shown that $Pd_{40}Ni_{40}P_{20}$[1] can be produced up to a thickness of 1 cm in its smallest dimension when the material was fluxed in B_2O_3. However, not until the 1990's did research intensify in this new area of ''bulk metallic glasses,'' when a new class of Zr based bulk metallic glasses[2,3] with potential applications was discovered. In particular, the alloy $Zr_{41.2}Ti_{13.8}Cu_{12.5}Ni_{10}Be_{22.5}$ (Vit1)[3] has an excellent glass forming ability that has initiated a series of crystallization studies over a wide temperature range below the melting temperature. A complete time–temperature–transformation (TTT) diagram for crystallization was measured by containerless electrostatic levitation (ESL) over the entire temperature range of the undercooled liquid, i.e., from the melting point down to the glass transition temperature, T_g.[4] This TTT diagram showed a typical ''C'' shape with the nose at 51 s and 850 K. The critical cooling rate to bypass crystallization was found to be 1.8 K/s. The TTT diagram could not be described by kinetic formulations as given, for example, by Uhlmann[5] and Davis.[6] This was attributed to the relatively complex crystallization behavior of Vit1, particularly at low temperatures where decomposition precedes nucleation.[7,8] The same TTT diagram as in Ref. 4, where the samples were processed without containers, was obtained from samples crystallized in graphite crucibles.[9] This method is more user friendly compared to ESL and has the advantage of a more reliable temperature reading.

Recently, the new Pd based bulk amorphous glass $Pd_{40}Cu_{30}Ni_{10}P_{20}$ (PCNP) was found,[10] which has a glass forming ability far exceeding that of $Pd_{40}Ni_{40}P_{20}$ and approaching or even exceeding that of Vit1. In contrast to Vit1, this Pd based alloy shows no decomposition on the nanometer scale at temperatures near T_g.[11]

In this letter, we report on crystallization studies of PCNP. Processing this alloy in graphite crucibles, using boron oxide flux, enabled us to measure the complete TTT diagram for crystallization in the undercooled melt and to determine the critical cooling rate. We present results of microstructure analysis of the PCNP melt after crystallization at temperatures near the nose of the TTT diagram. We further give a kinetic formulation which fits the TTT diagram over the entire range of the measurement.

Amorphous PCNP was produced by induction melting of Pd, $Cu_{73.4}P_{26.6}$, Ni_2P, and P in a silica tube of 10 mm diameter, using B_2O_3 oxide flux, and subsequent water quenching. For the crystallization studies, we used a differential thermal analysis (DTA) setup,[12] equipped with two graphite crucibles. The material was introduced to one of the crucibles, whereas the other was used as a reference. The crucibles were inductively heated in a titanium gettered argon atmosphere and their temperature was measured with type K thermocouples with an accuracy of ± 2 K. A control algorithm enabled us to perform isothermal anneals within ± 0.5 K of the setpoint. The microstructures of the solidified samples were analyzed with a Jeol JXA-733 electron microprobe equipped with five wavelength-dispersive x-ray (WDX) spectrometers, which allowed the element concentrations to be determined with an accuracy of ± 1 at. %.

The crystallization studies were performed on four PCNP samples with masses between 120 and 300 mg, processed in (less than 10 mg of) B_2O_3. The samples were heated up to 1173 K, i.e., 350 K above the liquidus temperature T_{liq} ($=823$ K, as measured by DTA), and subsequently cooled down with a rate of about 25 K/s to a selected temperature T. At that temperature, they were held isothermally until crystallization was detected, i.e., until a temperature rise owing to a release of heat of fusion (recalescence) was observed. These isothermal undercooling experiments were performed at different temperatures and are summarized in a TTT diagram, which is shown in Fig. 1 for temperatures between the glass transition temperature $T_g = 582$ K (as measured by differential scanning calorimetry with a heating rate of 10 K/min) and the liquidus temperature. The TTT diagram shows a C shape with the nose at 50 s and 680 K.

The results of the cooling experiments, performed with rates between 1.35 and 0.20 K/s, are shown in Fig. 2 (the inset gives an example for the sample processing). Recales-

[a]Electronic mail: loeffler@caltech.edu

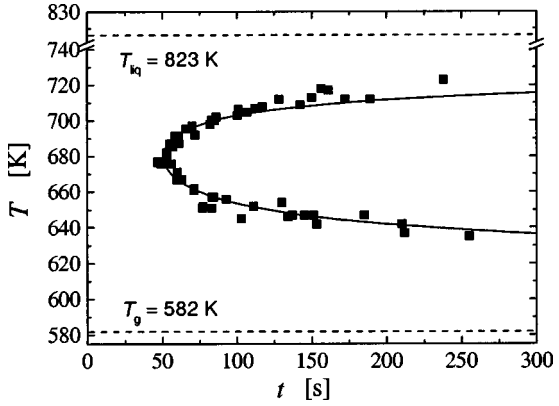

FIG. 1. Time–temperature–transformation (TTT) diagram for $Pd_{40}Cu_{30}Ni_{10}P_{20}$ (PCNP). The solid line describes the fit using the inverse function of $t(T)$, given in Eq. (3).

cence is observed for all cooling rates smaller than 0.33 K/s, whereas it is not observed for larger rates. Thus, the critical cooling rate of PCNP is about 0.33 K/s.

In order to determine the microstructure of the solidified samples, the four PCNP samples were quenched at certain temperatures and times, as given in the caption of Fig. 3; Figs. 3(a)–3(d) show electron backscattering images for these samples. All samples show a modulated structure in dark and light areas. To resolve the composition difference of this modulation, ''line scans'' were performed in which the local compositions in steps of 1 μm were investigated. Figures 3(e) and 3(f) give examples for the samples shown in Figs. 3(a) and 3(b). A modulated structure in Cu(rich)/P(poor) and Cu(poor)/P(rich) zones is observed. Since the beamsize of the WDX spectrometer is comparable with the distances over which the local compositions have been determined, the ''true'' absolute differences (in atomic percent) between the two zones will, however, be larger than those given in Figs. 3(e) and 3(f).

In addition, a distinct black phase can be observed in all samples [Figs. 3(a)–3(d)]. At 700 K, this black phase forms dendrites with sizes of up to 200 μm in length and 10 μm in thickness [Fig. 3(a)]. The WDX results show that this phase contains approximately three times as much Cu as Pd, with only little Ni and P. We, therefore, conclude that this phase is tetragonal Cu_3Pd, which was confirmed by x-ray diffraction. The vicinity around these dendrites (bright phase around the dendrite center) is enriched in Pd and poor in Cu, as detected by WDX.

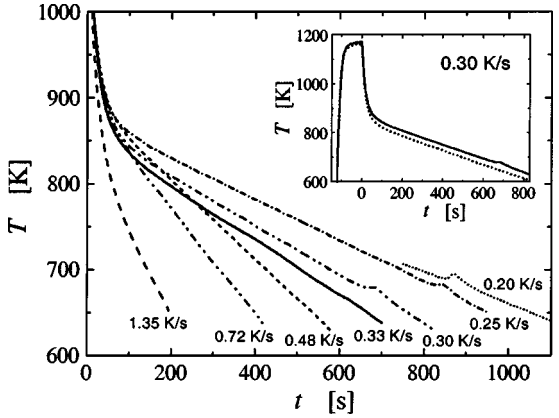

FIG. 2. Cooling diagram for PCNP. No recalescence is detected at cooling rates larger than 0.33 K/s. For lower rates, the onset of recalescence is visible at 670 K (0.30 K/s), 682 K (0.25 K/s) and 690 K (0.20 K/s). The inset illustrates the sample processing, showing the temperature (T)/time (t) profile of the reference (dotted line) and the sample (solid line) for a cooling rate of 0.30 K/s. Reference and sample are held for approximately 60 s at 1173 K (350 K above T_{liq}), free cooled to a temperature around T_{liq}, and then cooled with a rate as given.

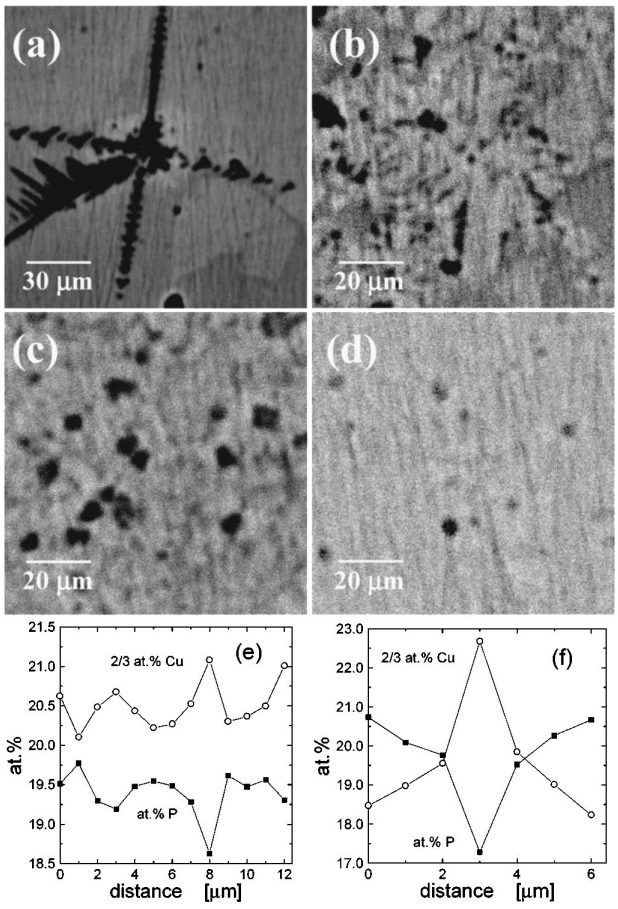

FIG. 3. Electron backscattering images of PCNP processed under different conditions; (a) quenched after 171 s at 700 K, (b) after 58 s at 677 K, (c) after 56 s at 677 K, and (d) after 129 s at 646 K. At all temperatures, a modulated structure in dark and light areas is observed; (e) and (f) illustrate the modulation for the samples shown in (a) and (b) by means of line scans in which the local compositions were investigated by WDX in steps of 1 μm. For a better illustration, the P composition (in atomic percent) is compared with two-thirds of the Cu composition.

At 677 K, the Cu/P modulated structure and the black phase are still present. A less pronounced dendrite structure as in Fig. 3(a) can be observed in Fig. 3(b), however, reduced in size to about 100 μm in length and 5 μm in thickness. The dendrite structure is not resolvable in Fig. 3(c), but the Cu_3Pd phase can still be detected. After quenching the sample below the ''nose'' temperature, the number density of the black phase is drastically reduced [Fig. 3(d)], the Cu/P modulated structure is, however, still observed.

The scanning electron microscopy pictures show that (despite a different morphology) the same primary phases form at the different degrees of undercooling. This is in contrast to Vit1, where at least three different primary solidified phases have been found for the different degrees of undercooling.[9] As such, the crystallization kinetics of PCNP seem to be less complicated than that of Vit1, although x-ray

diffraction performed on the four crystallized samples resolved additional Ni and Pd phosphides, and Pd_2Ni_2P.

In an attempt to describe the crystallization kinetics, we use, in the following, classical nucleation theory combined with a diffusion-controlled growth rate of the nuclei. In the classical theory (see, e.g., Ref. 13), the crystal nucleation rate per unit volume, I_ν, is,

$$I_\nu = \frac{A_\nu}{\eta(T)} \exp\left(- \frac{16\pi\sigma^3}{3k_B T[\Delta g(T)]^2} \right), \tag{1}$$

where A_ν is a constant of the order of 10^{32} Pa s/(m^3 s) for homogeneous nucleation, η is the viscosity, Δg is the difference in Gibbs free energy (per unit volume), k_B is the Boltzmann constant, and σ is the interfacial energy between the liquid and the nuclei. According to Ref. 14, the temperature dependence of η can be described by a Vogel–Fulcher–Tamman relation, $\eta(T) = \eta_0 \exp(D^* T_0/(T - T_0))$, with $\eta_0 = 9.34 \times 10^{-3}$ Pa s, $D^* = 9.25$, and $T_0 = 447$ K. The temperature dependence of Δg for the initial stages of the solidification was estimated using $\Delta g = \Delta S_F (T_{\text{liq}} - T)$,[15] where ΔS_F is the entropy of fusion (per volume of the liquid), and $T_{\text{liq}} = 823$ K. The growth of the nuclei was described by a diffusion-controlled mechanism, given by the product of a kinetic and thermodynamic factor,[5] i.e.,

$$u = \frac{k_B T}{3\pi l^2 \eta(T)} \left[1 - \exp\left(- \frac{n\Delta g(T)}{k_B T} \right) \right], \tag{2}$$

where n is the atomic volume and l is the (average) atomic diameter. In Eq. (2) the Stokes–Einstein equation has been used, which relates diffusivity and viscosity for temperatures above the glass transition (see, e.g., Refs. 5 and 16), i.e., $D = (k_B T)/(3\pi\eta l)$. Considering a steady state nucleation rate [Eq. (1)] and three-dimensional growth of the crystals (with no influence between the growing crystals), the time t to crystallize a detectable volume fraction x (of, for example, 0.5%) during isothermal annealing is

$$t = \left(\frac{3x}{\pi I_\nu(T)[u(T)]^3} \right)^{1/4}, \tag{3}$$

with $I_\nu(T)$ and $u(T)$ given by Eqs. (1) and (2), respectively. For the calculation of Δg, a value of $\Delta S_F = 8.55$ J/(mol K) is taken from Ref. 17. The (theoretical) atomic volume n for PCNP is 15.2 Å^3; the (theoretical) average atomic diameter is $l = 3.1$ Å. Thus, the only unknown parameters are the interfacial energy σ and the ''amplitude'' A_ν. The latter, however, does not change the shape of the TTT diagram. From the fit of Eq. (3) to the experimentally evaluated TTT diagram (see the solid line in Fig. 1), we obtain $\sigma = 0.067$ J/m^2 and $A_\nu = 4.4 \times 10^{31}$ Pa s/(m^3 s). The value of σ is comparable with values for monatomic liquids with similar melting temperatures, for example, $\sigma = 0.058$ J/m^2 for Cd ($T_{\text{liq}} = 594$ K) and 0.108 J/m^2 for Al ($T_{\text{liq}} = 933$ K).[18]

A similar procedure was used to fit the TTT diagram of Vit1.[19] There, however, no unique fit was obtained and the Stokes–Einstein relation held only for temperatures above $T = 850$ K. For lower temperatures, an Arrhenius-like effective diffusivity had to be used to describe the crystallization times. This gives evidence that the crystallization kinetics of PCNP and Vit1 are different at temperatures near T_g, in agreement with the results of Ref. 11.

Both systems, Vit1 and PCNP, crystallize at the nose temperature T_n after about 50 s. On the other hand, T_n is in PCNP much closer to T_g than in Vit1: for PCNP, $T_n = T_g + 0.41\Delta T_{\text{liq}}$, with $\Delta T_{\text{liq}} = T_{\text{liq}} - T_g = 241$ K; for Vit1, $T_n = T_g + 0.61\Delta T_{\text{liq}}$, with $\Delta T_{\text{liq}} = 370$ K. This difference can be explained by the different temperature dependencies of the viscosities, reported for PCNP in Ref. 14 and for Vit1 in Ref. 19. In an Angell plot, where $\ln \eta$ is plotted as a function of T_g/T, both viscosities show a crossover at $T_g/T = 0.77$, with (the more fragile) PCNP having the larger viscosity at high temperatures. This slows down the kinetics at high temperatures and thus lowers the nose temperature T_n compared to Vit1 (which has the larger viscosity at low temperatures).

In summary, PCNP is a new bulk glass forming alloy with an exceptionally high glass forming ability and a critical cooling rate of 0.33 K/s. Isothermal crystallization studies show a modulation in Cu and P for all degrees of undercooling and a primary solidified phase of Cu_3Pd. A complete TTT diagram was obtained for this alloy and successfully described by combining steady state nucleation and diffusion-controlled growth (governed by the Stokes–Einstein relation) for all degrees of undercooling. This is in contrast to the behavior of many bulk glass forming systems, in which decomposition precedes nucleation at low temperatures and thus limits their thermal stability. The exceptional glass-forming ability of PCNP presumably results from the exceptionally high reduced glass transition temperature of 0.71 and from the sluggish kinetics at high temperatures.

This work was supported by the U.S. Department of Energy (Grant No. DEFG-03-86ER45242). Partial support for J.L. was provided by the Alexander von Humboldt Foundation via the Feodor Lynen Program.

[1] H. W. Kui, A. L. Greer, and D. Turnbull, Appl. Phys. Lett. **45**, 615 (1984).
[2] T. Zhang, A. Inoue, and T. Masumoto, Mater. Trans., JIM **32**, 1005 (1991).
[3] A. Peker and W. L. Johnson, Appl. Phys. Lett. **63**, 2342 (1993).
[4] Y. J. Kim, R. Busch, W. L. Johnson, O. J. Rulison, and W. K. Rhim, Appl. Phys. Lett. **68**, 1057 (1996).
[5] D. R. Uhlmann, J. Non-Cryst. Solids **25**, 43 (1977).
[6] H. A. Davis, Phys. Chem. Glasses **17**, 159 (1976).
[7] R. Busch, S. Schneider, A. Peker, and W. L. Johnson, Appl. Phys. Lett. **67**, 1544 (1995).
[8] J. F. Löffler and W. L. Johnson, Appl. Phys. Lett. **76**, 3394 (2000).
[9] J. Schroers, R. Busch, A. Masuhr, and W. L. Johnson, Appl. Phys. Lett. **74**, 2806 (1999).
[10] A. Inoue, N. Nishiyama, and H. Kimura, Mater. Trans., JIM **38**, 179 (1997).
[11] J. F. Löffler, W. L. Johnson, W. Wagner, and P. Thiyagarajan, Mater. Sci. Forum **343–346**, 179 (2000).
[12] A. Masuhr, Ph.D. thesis, California Institute of Technology, 1999.
[13] D. M. Herlach, Mater. Sci. Eng. R **12**, 177 (1994).
[14] N. Nishiyama and A. Inoue, Acta Mater. **47**, 1487 (1999).
[15] H. I. Aaronson, K. R. Kinsman, and K. C. Russell, Scr. Metall. **4**, 101 (1970), give an expression for Δg when there is a composition change between the (crystallizing) solid and the liquid, resulting in a time-dependent Δg. However, in the present initial stages, the small volume fraction of the nuclei only slightly changes the composition of the liquid.
[16] J. Jäckle, Rep. Prog. Phys. **49**, 171 (1986).
[17] I.-R. Lu, G. Wilde, G. P. Görler, and R. Willnecker, J. Non-Cryst. Solids **250–252**, 577 (1999).
[18] K. F. Kelton, Solid State Phys. **45**, 75 (1991).
[19] A. Masuhr, T. A. Waniuk, R. Busch, and W. L. Johnson, Phys. Rev. Lett. **82**, 2290 (1999).